Prediction of disclinations in nematic elastomers

Eliot Fried[†] and Russell E. Todres

Department of Theoretical and Applied Mechanics, University of Illinois, Urbana, IL 61801-2935

Edited by Howard Brenner, Massachusetts Institute of Technology, Cambridge, MA, and approved October 23, 2001 (received for review July 27, 2001)

We present a theory for uniaxial nematic elastomers with variable asphericity. As an application of the theory, we consider the time-independent, isochoric extension of a right circular cylinder. Numerical solutions to the resulting differential equation are obtained for a range of extensions. For sufficiently large extensions, there exists an isotropic core of material surrounding the cylinder axis where the asphericity vanishes and in which the polymeric molecules are shaped as spherical coils. This region, corresponding to a disclination of strength +1 manifesting itself along the axis, is bounded by a narrow transition layer across which the asphericity drops rapidly and attains a nontrivial negative value. Away from the disclination, the material is anisotropic, and the polymeric molecules are shaped as ellipsoidal coils of revolution oblate about the radial direction. Along with the area of steeply changing asphericity between isotropic and anisotropic regimes, a marked drop in the free-energy density is observed. The boundary of the disclination core is associated with the location of this energy drop. For realistic choices of material parameters, this criterion yields a core on the order of 10^{-2} μm, which coincides with observations in conventional liquid crystal melts. Finally, we find that the total energy definitively shows a preference for disclinated states.

As technological applications of liquid crystals have grown over the past 30 years, so, too, has research into the structure and importance of their defects. Initially, defect-induced disruptions were the bane of liquid crystal displays. Now though, as Mottram and Sluckin (1) observe, these very defects are being harnessed in the zenithal bistable display. Also, as shown by Chandrasekhar (2) and Kléman (3), the presence of defects is necessary for the stabilization of some of the blue phases observed in cholesteric liquid crystals. In addition, recent research by Mottram and Sluckin (1), Adrienko and Allen (4), and Mottram and Hogan (5) has shown the important effect of disclinations on the phase transition behavior in nematic liquid crystals. Because point, line, and surface defects manifest themselves in liquid crystals, as noted by Kléman (3), their study has enhanced the understanding of defects in other media.

A disclination in a nematic liquid crystal is a line along which the director is undefined. In the Oseen–Zöcher–Frank (OZF) theory [Oseen (6), Zöcher (7), Frank (8)], a nonintegrable singularity in the free-energy density occurs at a disclination. Historically, this difficulty was addressed by positing a core of fixed radius and energy about the disclination. Both Mottram and Hogan (5) and Ericksen (9) observe though that the fixed-energy approach gives no information about the magnitude and energy of the core and also fails to elucidate the underlying physical nature of the core. Nevertheless, for nematics confined to capillaries, it has been shown by Williams *et al.* (10) that the director can "escape into the third dimension" at the singularity, thus obviating the need for a core but not necessarily ruling one out altogether. This deficiency of the OZF theory led Ericksen (9) to develop a regularized theory involving the degree of orientation, a scalar field that vanishes at disclinations and enters the free energy density in a manner that mollifies the singularity otherwise associated with a disclination. Exploiting this idea, Mottram and Sluckin (1), Adrienko and Allen (4), and Mottram and Hogan (5) have obtained values of the core radius and energy of a disclination in a cylindrical configuration.

Here, we study disclinations in nematic elastomers. These materials differ from melts in that the polymer chains in the elastomer are cross-linked. The nematic mesogens may still be either main chain or pendant, as in a melt. Nematic and other optically active polymers are of ever growing interest, as is attested by the reviews of Finkelmann (11), Zentel (12), Davis (13), Warner and Terentjev (14), and Terentjev (15), and the recent work on artificial muscles by deGennes *et al.* (16) and on tunable lasers by Finkelmann *et al.* (17). Our effort is motivated by the belief that the understanding of disclinations and other defects in optically active polymers such as nematic elastomers is of fundamental importance and will have far-reaching technological consequences.

Model

We envision the elastomer to be formed in a two-step process. First, the nematic melt is cross-linked in a uniaxial state, i.e., one in which the average molecular conformation of the polymeric molecules at each material point assumes the shape of an ellipsoid of revolution with asphericity $q_* > -1$. An annealing process is then performed. This process randomizes the orientation of nematic mesogens and results in an isotropic state—taken to be our reference state—wherein the conformation at each material point is spherical.

To describe such a material, we consider a simplification and simultaneous extension of the molecular-statistical free-energy density of Warner, Gelling, and Vilgis (18). The simplification stems from restricting conformations to the uniaxial case and taking the reference state to be isotropic. On the other hand, the extension follows from including a term analogous to that arising in the OZF theory and terms associated with the degree of asphericity of the ellipsoids of revolution. These include a double-well potential in the asphericity and a regularizing term quadratic in the gradient of the asphericity. The double-well potential isolates as preferred not only the isotropic reference state but also those states with asphericity q_*. In this sense, the material "remembers" the asphericity present at the instant of cross-linking. Specifically, the free-energy density has the form

$$\frac{\mu}{2}\left((1+q)^{\frac{1}{3}}\left(|\boldsymbol{F}|^2-\frac{q}{1+q}|\boldsymbol{F}^{\top}\boldsymbol{n}|^2\right)-3\right)$$

$$+\Phi(q)+\frac{\alpha}{2}|\boldsymbol{h}|^2+\Gamma(q)K(\boldsymbol{F},\boldsymbol{n},\boldsymbol{G}), \qquad [1]$$

where $\boldsymbol{F}$ is the deformation gradient, subject to the constraint $\det\boldsymbol{F}=1$ of incompressibility; $q>-1$ is the asphericity (the case of $-1<q<0$ corresponds to average molecular conformation having the shape of an oblate ellipsoid of revolution about $\boldsymbol{n}$, while prolate ellipsoids of revolution about $\boldsymbol{n}$ are described by

This paper was submitted directly (Track II) to the PNAS office.

Abbreviation: OZF, Oseen–Zöcher–Frank.

[†]To whom reprint requests should be addressed. E-mail: e-fried@uiuc.edu.

The publication costs of this article were defrayed in part by page charge payment. This article must therefore be hereby marked "*advertisement*" in accordance with 18 U.S.C. §1734 solely to indicate this fact.

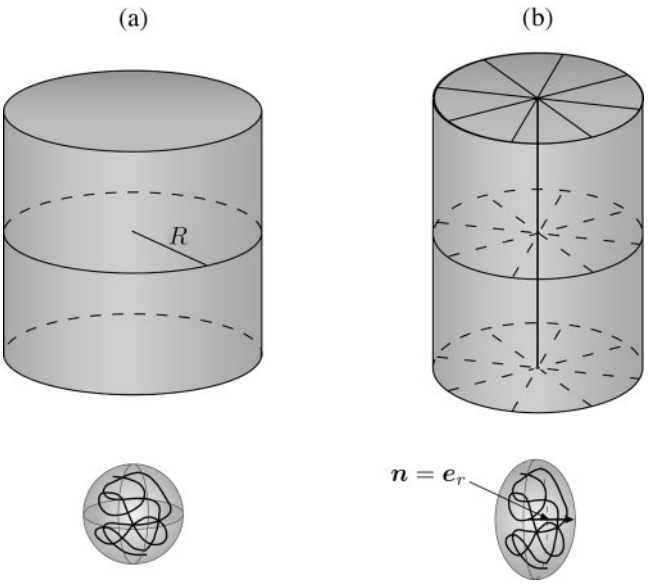

Fig. 1. Cylinder and molecular conformation in undistorted (*a*) and distorted (*b*) states.

$q > 0$); $\boldsymbol{h} = \text{Grad}\, q$ is the asphericity gradient; $\boldsymbol{n}$ is the nematic director of unit magnitude; and $\boldsymbol{G} = \text{Grad}\, \boldsymbol{n}$ is the director gradient. In addition, we have $\mu > 0$, the rubber-elasticity modulus; Φ, a double-well potential, consistent with

$$\left.\begin{aligned} &\Phi(0) = \Phi(q_*) = 0, \\ &\Phi(q) > 0 \qquad \text{for } q \neq 0, q_*, \\ &\Phi(q) \to +\infty \quad \text{as } q \to -1, +\infty; \end{aligned}\right\} \qquad [2]$$

$\alpha > 0$, a regularizing modulus; Γ, a mollifying factor, dimensionless and consistent with

$$\left.\begin{aligned} &\Gamma(q) = O(q^2) \qquad \text{as } q \to 0, \\ &\Gamma(q) > 0 \qquad \text{for } q \neq 0, \\ &\Gamma(q) \to +\infty \qquad \text{as } q \to -1, +\infty; \end{aligned}\right\} \qquad [3]$$

and generalization

$$\begin{aligned} K(\boldsymbol{F}, \boldsymbol{n}, \boldsymbol{G}) = {} & \kappa_1(\boldsymbol{F} \cdot \boldsymbol{G})^2 + \kappa_2|\boldsymbol{F}^\top \boldsymbol{G}|^2 \\ & + \kappa_3(\boldsymbol{F}^\top \boldsymbol{G})\cdot(\boldsymbol{G}^\top \boldsymbol{F}) \\ & + \kappa_4(|\boldsymbol{F}^\top \boldsymbol{G}\boldsymbol{F}^\top \boldsymbol{n}|^2 + |\boldsymbol{G}^\top \boldsymbol{F}\boldsymbol{F}^\top \boldsymbol{n}|^2) \\ & + \kappa_5(\boldsymbol{F}^\top \boldsymbol{G}\boldsymbol{F}^\top \boldsymbol{n})\cdot(\boldsymbol{G}^\top \boldsymbol{F}\boldsymbol{F}^\top \boldsymbol{n}) \end{aligned} \qquad [4]$$

of the OZF energy-density, involving orientational-elasticity moduli $\kappa_1 > 0$, $\kappa_2 > 0$, $\kappa_3 > 0$, $\kappa_4 > 0$, and $\kappa_5 > 0$. On setting $\boldsymbol{F} = \boldsymbol{1}$ in Eq. **4**, we may identify $\kappa_1 + \kappa_2 + \kappa_4$, κ_2, $\kappa_2 + \kappa_3$, and $\kappa_2 + \kappa_4$ with the classical splay, twist, bend, and saddle-splay moduli of the OZF theory; $\kappa_4 + \kappa_5$ is an additional saddle-splay modulus that accounts for interactions between the distortion of network cross-links and the orientation of the molecular agglomeration. Both Φ and Γ penalize states in which the asphericity tends toward the extreme values $q = -1$ and $q = \infty$.

We use Eq. **1** to investigate the presence of disclinations of strength $+1$ in a cylindrical, nematic-elastomeric specimen of radius R and length L subjected to an isochoric deformation with gradient

$$\boldsymbol{F} = Ae_r \otimes e_r + Ae_\theta \otimes e_\theta + \frac{1}{A^2} e_z \otimes e_z, \qquad [5]$$

where $A > 0$ is the ratio of the deformed to undeformed cylinder radius (Fig. 1). Hence, values of A between zero and unity correspond to extension of the cylinder along its axis while those greater than unity correspond to contraction. We limit our study solely to the case of extension, although similar results are expected for compression. We suppose that the director is either radial, namely

$$\boldsymbol{n} = e_r, \qquad [6]$$

or, as would be the case when $q = 0$, undefined. Further, we suppose that the asphericity depends at most on the radial coordinate r.

Using Eqs. **5** and **6** gives

$$K(\boldsymbol{F}, \boldsymbol{n}, \boldsymbol{G}) = \frac{\kappa A^2}{r^2}, \qquad [7]$$

with $\kappa = \kappa_1 + \kappa_2 + \kappa_3$, the orientational-splay modulus. See the discussion following Eq. **4**.

Furthermore, introducing $x = r/R$, $Q(x) = q(Rx)$, and ν, a parameter proportional to the height of the barrier separating the minima of the double-well potential Φ, we obtain the dimensionless groups

$$\mu^* = \frac{\mu}{\nu}, \ \kappa^* = \frac{\kappa}{R^2\nu}, \text{ and } \alpha^* = \frac{\alpha}{R^2\nu}. \qquad [8]$$

In view of our assumptions concerning $\boldsymbol{F}$, $\boldsymbol{n}$, and q, we arrive at the dimensionless specialization

$$\Psi = \Psi_e + \Psi_a + \Psi_o \qquad [9]$$

of the free-energy density, with

$$\Psi_e = \frac{\mu^*}{2}\left(2A^2 + \frac{1}{A^4} - 3\right), \qquad [10]$$

a conventional neo-Hookean rubber-elastic contribution associated with the distortion of network cross-links,

$$\begin{aligned} \Psi_a = {} & \frac{\mu^*}{2}\left(A^2\left(\frac{2+Q}{(1+Q)^{\frac{2}{3}}} - 2\right) + \frac{1}{A^4}\left((1+Q)^{\frac{1}{3}} - 1\right)\right) \\ & + \frac{\Phi(Q)}{\nu} + \frac{\alpha^*}{2}\left(\frac{dQ}{dx}\right)^2 \end{aligned} \qquad [11]$$

a contribution associated with the asphericity of the molecular agglomeration, and

$$\Psi_o = \frac{\kappa^* A^2 \Gamma(Q)}{2x^2} \qquad [12]$$

a contribution associated with the axis about which the molecular agglomeration is oriented.

In equilibrium, the form of the asphericity is governed by the Euler–Lagrange equation

$$\frac{\alpha^*}{x}\frac{d}{dx}\left(x\frac{dQ}{dx}\right) = M(Q, x) \qquad [13]$$

and the natural boundary conditions

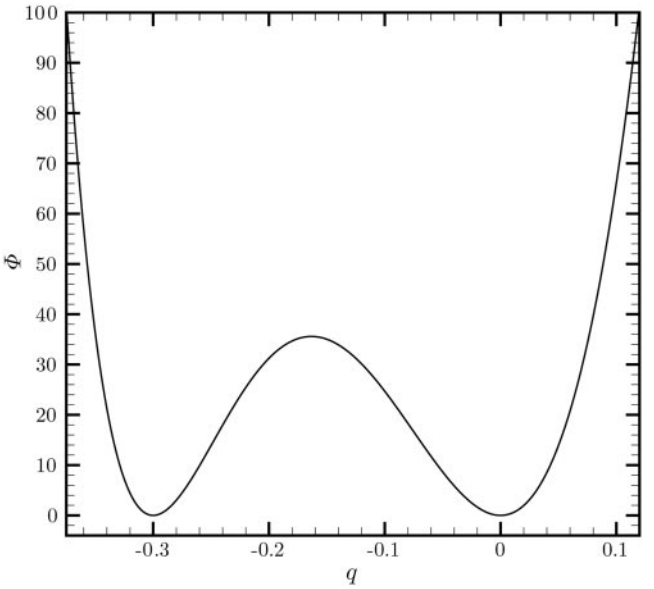

Fig. 2. Plot of Φ, as defined in Eq. **16** with $\nu = 10^5$ J/m^3 and $q_* = -0.3$.

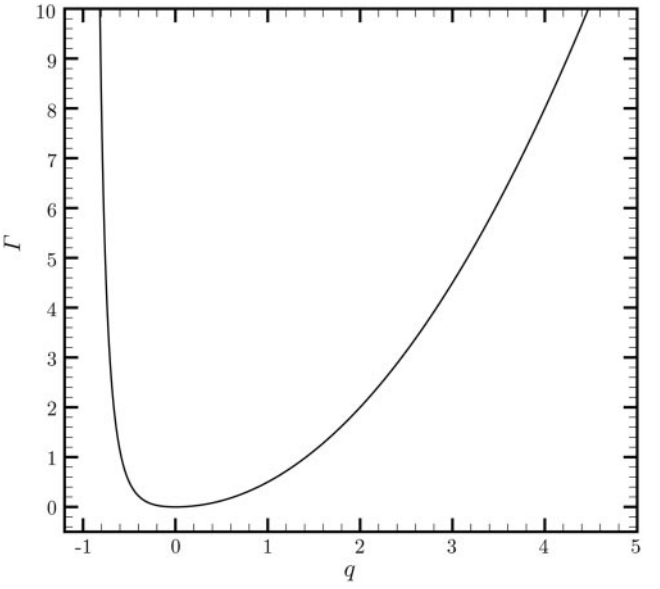

Fig. 3. Plot of Γ, as defined in Eq. **17**.

$$\alpha^* \left.\frac{dQ}{dx}\right|_{x=0} = \alpha^* \left.\frac{dQ}{dx}\right|_{x=1} = 0, \qquad [14]$$

with M given by

$$M(Q,x) = \frac{\mu^* A^2}{6(1+Q)^{\frac{2}{3}}}\left(\frac{1}{A^6} - \frac{1-Q}{1+Q}\right) + \frac{\kappa^* A^2 \Gamma'(Q)}{x^2} + \frac{\Phi'(Q)}{\nu}. \qquad [15]$$

Numerical Results

The differential equation **13** involves functions Φ and Γ, which are restricted only by Eqs. **2** and **3**. For our numerical investigation, we took

$$\Phi(q) = \frac{\nu q^2 (q-q_*)^2}{2(1+q)^2}, \qquad [16]$$

where, as stated before, $\nu > 0$ determines the height of the energy barrier between states with $q = 0$ and $q = q_*$ (Fig. 2), and

$$\Gamma(q) = \begin{cases} \dfrac{q^2}{2(1+q)^2} & \text{if } -1 < q \le 0, \\ \dfrac{q^2}{2} & \text{if } q \ge 0. \end{cases} \qquad [17]$$

While defined piecewise, this choice of Γ (Fig. 3) is twice continuously differentiable. Thus, because Γ′ appears in Eq. **13**, we expect no numerical complications caused by this choice.

Because we restrict our attention to extension ($0 < A < 1$), we expect an elongation of the molecular agglomeration parallel to the cylinder axis during extension. Thus, it is only natural to restrict q_* to lie between 0 and −1. Otherwise, there would be no reason for a disclination to form. However, considering the case of cylinder compression ($A > 1$), the molecular agglomeration would be prolate in the radial direction, and we would, therefore, choose $q_* > 0$.

The boundary-value-problem (Eqs. **13** and **14**) was solved numerically by using the ACDC package of Cash and Wright (19) with the tolerance on the solution of Q set to 10^{-8} and that of its derivative dQ/dx set to 10^{-4}. In so doing, we set $\mu = \nu = 10^5$ J/m^3, $\kappa = \alpha = 10^{-11}\, J/m$, *and* $R = 1$ cm. The values of μ and κ are realistic and in line with those used by Verwey, Warner, and Terentjev (20) in their work on stripes in nematic elastomers. As a result of these choices, $\mu^* = 1$ and $\kappa^* = \alpha^* = 10^{-12}$. Further, for illustrative purposes, we took $q_* = -0.3$. As our initial, trial solution, we used the straight line $Q = 0$, satisfying Eq. **14** and consisting of 501 evenly spaced points on the closed domain. The only parameter varied was A, the degree of cylinder distortion, which we allowed to range between 0.86 and 1. Fig. 4 shows a sharp transition between isotropic ($q = 0$) and

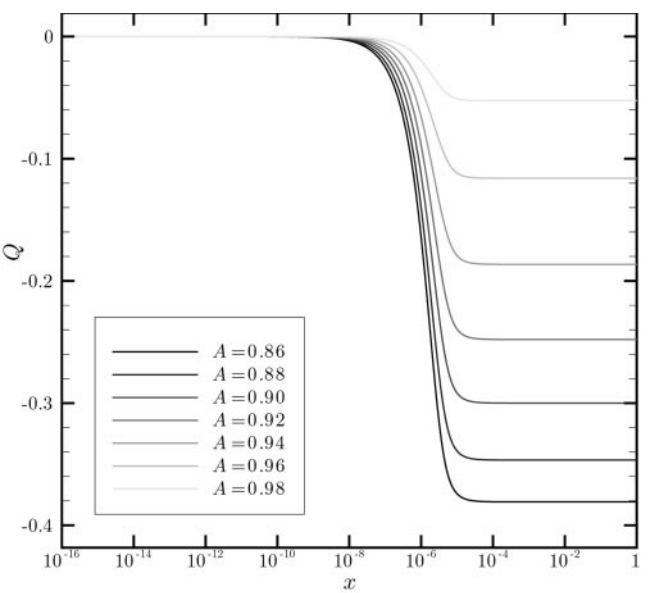

Fig. 4. Plots of the asphericity Q as a function of dimensionless radial position x (note logarithmic scale) for representative values of the degree A of cylinder distortion between 0.86 and 1. Consistent with Eq. **14**, note the horizontal slopes at the cylinder center ($x = 0$) and outer boundary ($x = 1$).

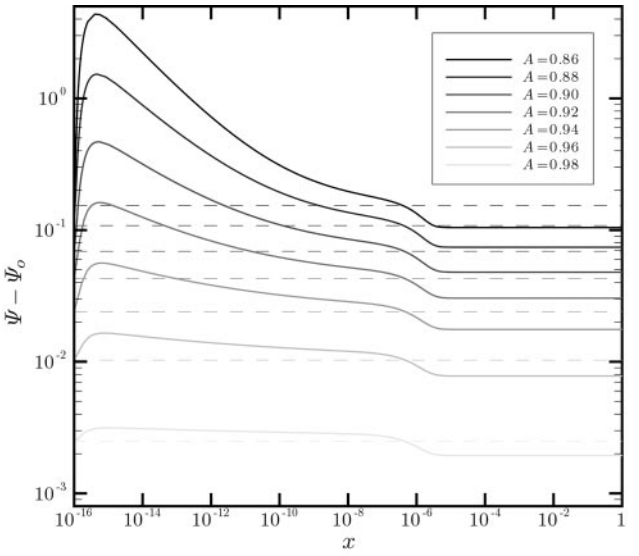

Fig. 5. Plots of the contributions of $\Psi - \Psi_o$ (solid lines) and Ψ_e (dashed lines) to the free-energy density as a function of dimensionless radial position x (note logarithmic scale) for the dimensionless material parameters $\mu^* = 1$, $\kappa^* = \alpha^* = 10^{-12}$, and $q_* = -0.3$ and representative values of the degree A of cylinder distortion between 0.86 and 1.

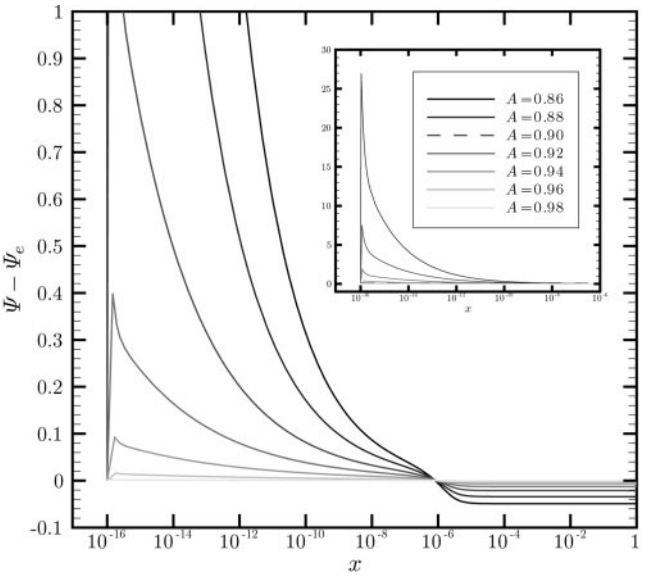

Fig. 6. Plots of the portion $\Psi - \Psi_e$ of the free-energy density, excluding the rubber-elastic contribution, as a function of dimensionless radial position x (note logarithmic scale) for the dimensionless material parameters $\mu^* = 1$, $\kappa^* = \alpha^* = 10^{-12}$, and $q_* = -0.3$ and representative values of the degree A of cylinder distortion between 0.86 and 1.

anisotropic ($q \neq 0$) regions along the cylinder radius, thereby indicating the presence of a disclination. Following Mottram and Hogan (5), the extent of the core can be inferred from the plot as the region where Q exhibits a rapid decrease. From Fig. 4, the center of the transition zone appears to be at $x = 10^{-6}$, which corresponds to a dimensional core radius on the order of 10^{-2} μm and is consistent with the length scale predicted by the ratio $\sqrt{\kappa/\mu} = \sqrt{\kappa/\nu}$ for our choices of μ, ν, and κ. A closer examination of the solution curves places the center of the layer at $x = 1.5 \times 10^{-6}$ (corresponding to a core radius of 0.015 μm), which we associate with the core boundary and denote by x_c. Our core radius is of the same order as values reported by Chandrasekhar and Ranganath (21) for liquid crystalline melts.

For each A, the contributions, Ψ_e and $\Psi - \Psi_o$, to the dimensionless free-energy density of Eq. **9**, which are unassociated with the axis of orientation of the molecular agglomeration, are shown in Fig. 5. The difference $\Psi - \Psi_e$, which includes all terms of Eq. **9** unrelated to the neo-Hookean distortion of the network cross-links is plotted in Fig. 6. We see from Figs. 5 and 6 that the free-energy density has markedly different behavior below and above x_c. This confirms our initial estimate of the core region from Fig. 4. From Fig. 5, Ψ_e is constant across the entire domain, while for corresponding values of extension, $\Psi - \Psi_o$ is greater than Ψ_e inside the core but less without. We note that the difference between Ψ_e and $\Psi - \Psi_o$ increases with greater extension away from the core. In the same region, we see from Fig. 6 that $\Psi - \Psi_e$ decreases with increasing extension. Taken together and noting that the core is only a small part of the domain, these trends presage that the total neo-Hookean energy

$$\mathcal{F}_e^{\text{tot}} = \int_0^1 \Psi_e(x) x dx \qquad [18]$$

will always be greater than the total energy

$$\mathcal{F}^{\text{tot}} = \int_0^1 \Psi(x) x dx \qquad [19]$$

and that their difference will grow with increasing extension.

In fact, the free-energy totals $\mathcal{F}_e^{\text{tot}}$ and $\mathcal{F}^{\text{tot}}$ shown in Fig. 7 do indeed bear this out. We note an expected monotonic increase of both $\mathcal{F}_e^{\text{tot}}$ and $\mathcal{F}^{\text{tot}}$ with increasing cylinder elongation (decreasing A). Also, as we surmised earlier, for all extension ratios, $\mathcal{F}^{\text{tot}}$ is less than $\mathcal{F}_e^{\text{tot}}$, the neo-Hookean contribution alone. From Fig. 4, all extensions give rise to a nontrivial asphericity at $x \gtrsim 10^{-6}$. Therefore, the results from Fig. 7 show that for any extension ratio, there is an energetic motivation for the material not to remain isotropic but to form a disclinated region with the remainder of the domain in an anisotropic state. This incentive

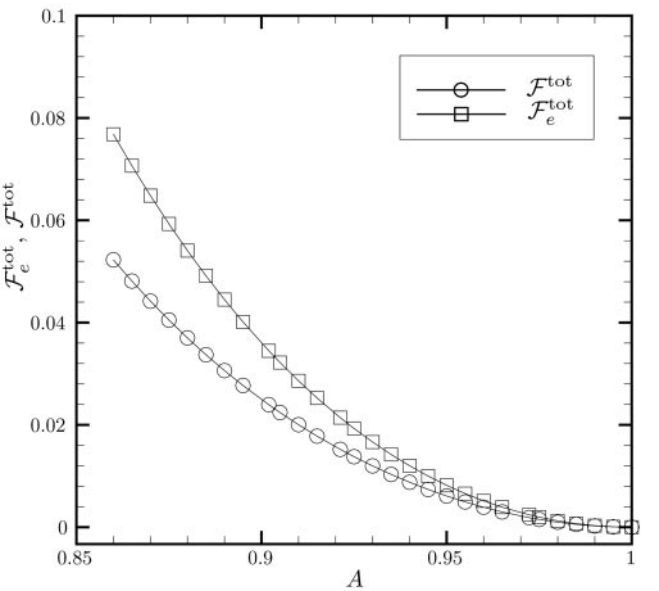

Fig. 7. Plots of the total neo-Hookean rubber-elastic energy $\mathcal{F}_e^{\text{tot}}$ and of the total free-energy $\mathcal{F}^{\text{tot}}$ as a function of the degree A of cylinder distortion between 0.86 and 1 for the dimensionless material parameters $\mu^* = 1$, $\kappa^* = \alpha^* = 10^{-12}$, and $q_* = -0.3$.

becomes stronger as the extension increases, as indicated by the growth of $\mathcal{F}_e^{\text{tot}} - \mathcal{F}^{\text{tot}}$ with extension, shown in Fig. 7. The lack of a threshold value of extension below which the isotropic state is preferred and above which a disclinated one is favored can be attributed to the fact that the well heights of Φ in Fig. 2 are equal. If the well corresponding to $q = 0$ was lower than that for $q = q_*$ we would expect a threshold, with extent depending on the height difference between the wells. On the other hand, a threshold would still be absent if the well corresponding to $q = 0$ was higher than that for $q = q_*$.

In addition, we investigated the energy of the core, which we denote as

$$\mathcal{F}^{\text{core}} = \int_0^{x_c} \Psi(x) x dx, \qquad [20]$$

relative to that of the whole domain. From Fig. 8, it is evident that $\mathcal{F}^{\text{core}}$ is a vanishingly small percentage of $\mathcal{F}^{\text{tot}}$. This is because of the relatively small size of the core and the fact that Ψ_e is of a comparatively large magnitude across the entire domain. However, we see that the core becomes energetically more important with increasing extension for most of our range until $A \approx 0.875$. For greater values of extension ($A \lesssim 0.875$), the core becomes energetically less important as more energy goes into both stretching of the network cross-links and changing the asphericity of the molecules comprising the network.

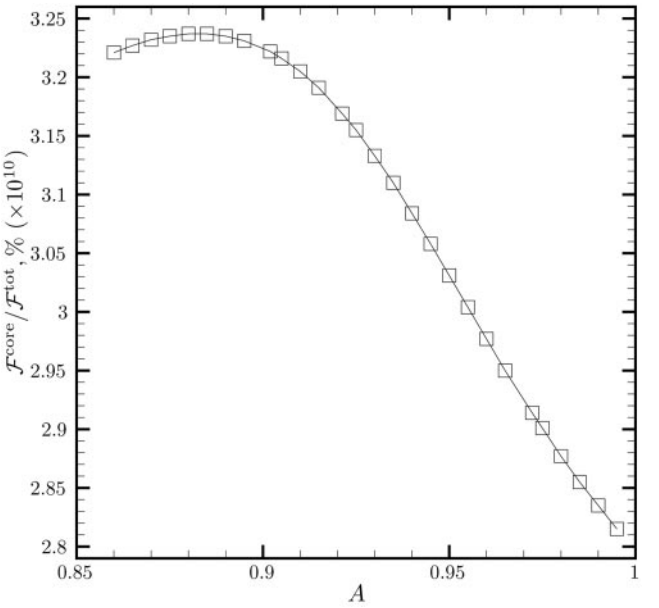

Fig. 8. Plot of the percentage $\mathcal{F}^{\text{core}}/\mathcal{F}^{\text{tot}}$ of free energy in the core as a function of the degree A of cylinder distortion between 0.86 and 1 for the dimensionless material parameters $\mu^* = 1$, $\kappa^* = \alpha^* = 10^{-12}$, and $q_* = -0.3$.

Discussion

As with any important class of new materials such as nematic elastomers, to proceed with applications designed to take complete advantage of their unique properties requires a thorough theoretical understanding of their behavior. In this spirit and working within a rigorous theoretical framework, we predict the existence of disclinations in nematic elastomers. We also obtain information concerning the characteristic dimension of a disclination core and the distribution of energy in disclinated states. We show that there is an energetic reason for the material to become disclinated as opposed to remaining isotropic as would a conventional neo-Hookean rubber. Because disclinations have been found to be so important in conventional liquid crystals, it is also likely that this will be the case in nematic elastomers. While our predictions are confined to nematic elastomers that have been specially prepared, we speculate that disclinations may occur under other circumstances. We hope that this work leads to further study in this area and, especially, to experiments designed to test our predictions.

1. Mottram, N. J. & Sluckin, T. J. (2000) *Liquid Crystals* **27,** 1301–1304.
2. Chandrasekhar, S. (1988) *Contemp. Phys.* **29,** 527–558.
3. Kléman, M. (1989) *Rep. Prog. Phys.* **52,** 555–654.
4. Adrienko, D. & Allen, M. P. (2000) *Phys. Rev. E* **61,** 504–510.
5. Mottram, N. J. & Hogan, S. J. (1997) *Philos. Trans. R. Soc. London A* **355,** 2045–2064.
6. Oseen, W. C. (1933) *Trans. Faraday Soc.* **29,** 883–899.
7. Zöcher, H. (1933) *Trans. Faraday Soc.* **29,** 945–957.
8. Frank, F. C. (1958) *Discuss. Faraday Soc.* **25,** 19–28.
9. Ericksen, J. L. (1991) *Arch. Rat. Mech. Anal.* **113,** 97–120.
10. Williams, C., Pierański, P. & Cladis, P. E. (1972) *Phys. Rev. Lett.* **29,** 90–92.
11. Finkelmann, H. (1988) *Angew. Chem.* **100,** 1019–1020.
12. Zentel, R. (1989) *Angew. Chem. Adv. Mater.* **101,** 1437–1445.
13. Davis, F. J. (1993) *J. Mater. Chem.* **3,** 551–562.
14. Warner, M. & Terentjev, E. M. (1996) *Progr. Polymer Sci.* **21,** 853–891.
15. Terentjev, E. M. (1999) *J. Phys. Condens. Matter* **11,** R239–R257.
16. de Gennes, P. G., Hebert, M. & Kant, R. (1997) *Macromol. Symp.* **113,** 39–49.
17. Finkelmann, H., Kim, S. T., Munoz, A., Palffy-Muhoray, P. & Taheri, B. (2001) *Adv. Materials* **13,** 1069–1072.
18. Warner, M., Gelling, K. P. & Vilgis, T. A. (1988) *J. Chem. Phys.* **88,** 4008–4013.
19. Cash, J. R. & Wright, R. W. (1998) *Appl. Numer. Math.* **28,** 227–244.
20. Verwey, G. C., Warner, M. & Terentjev, E. M. (1996) *J. Phys. II* **6,** 1273–1290.
21. Chandrasekhar, S. & Ranganath, G. S. (1986) *Adv. Phys.* **35,** 507–596.